Electron transport and intrinsic mobility limits in two-dimensional electron gases of III-V nitride heterostructures

Debdeep Jena* Yulia Smorchkova, Chris Elsass, Arthur C. Gossard, and Umesh K. Mishra
Department of Electrical and Computer Engineering, University of California, Santa Barbara, CA 93106

Electron transport studies for AlGaN/GaN two-dimensional electron gases is presented. Novel defects in the III-V nitrides are treated theoretically for two-dimensional transport. Theory of electron scattering by charged dislocation lines is presented for realistic two-dimensional electron gases. The theory lets us draw new conclusions about the nature of charges residing in the dislocation in the III-V nitrides. The theory leads to the recognition of the fact that current state of the art highest mobility values are limited intrinsically and not due to removable defects. Ways of bypassing the intrinsic limits to achieve higher mobilities are proposed.

I. INTRODUCTION

Over the last decade, the III-V nitrides have matured as a technologically important semiconductor system. Various optoelectronic products based on the nitrides have already gone commercial[1,2]; the material system holds abundant promise for more. Along with the technological importance, the nitrides offer a rich diversity of new physical phenomena such as large polarization fields and large band offsets[3]. These novel phenomena present a new way of creating two-dimensional electron gases (2DEGs) at heterointerfaces - without intentional modulation doping. M-Plane growth on tetragonal $LiAlO_2$ has been achieved[4], thus giving the experimentalist control over polarization fields. Recently, integral as well as fractional quantum hall effects have been observed in AlGaN/GaN 2DEGs, confirming that the 2DEGs are of high purity[5].

However the measured electron mobilities are still much lower than their counterparts in the AlGaAs/GaAs 2DEGs[6]. It is now well known that low temperature electron mobility in the purest AlGaAs/GaAs 2DEGs is limited by Coulombic scattering by remote ionized donors[7]. However, 2DEGs in AlGaN/GaN have been created without any intentional modulation doping; still the low temperature electron mobilities are much lower than the AlGaAs/GaAs 2DEGs. We present a detailed analysis of transport in the AlGaN/GaN 2DEG, and pinpoint the sources of scattering that are currently limiting low temperature electron mobilities.

II. 2DEG TRANSPORT THEORY

We first determine the transport regime to choose the correct theoretical treatment. Low-temperature transport in the nitride heterostructure 2DEGs is characterized by long mean free paths; typical numbers are $L \approx 0.5\mu m$ for a 2DEG of density $n_{2D} = 10^{13}/cm^2$ and $\mu = 10,000 cm^2/V.s$. The Ioffe-Regel criterion $k_F L >> \frac{1}{2\pi}$ is exceeded many times over, which is characteristic of diffusive rather than hopping transport.

We point out an interesting fact : the characteristic dimensionless parameter $r_s = E_{e-e}/E_F$ (the ratio of electron-electron potential energy and the kinetic energy), which is a measure of the importance of many-particle interactions, ranges from $r_s = 0.2$ for AlGaN/GaN 2DEG density $n_{2D} = 10^{13}/cm^2$ to $r_s = 2$ for 2DEG density $n_{2D} = 10^{12}/cm^2$. This means that for AlGaN/GaN 2DEGs with low 2DEG densities, many body effects such as exchange and interaction can play important effects. This sensitivity stems from the relatively heavy electron effective mass ($m^* = 0.2m_0$, m_0 being the free electron mass) compared to other III-V semiconductors. However, electron-electron scattering is elastic. Drift in response to applied external fields cannot be impeded by this form of scattering, since energy lost by one electron in a scattering event is gained by the other and both electrons contribute to the drift current. When combined with other scattering mechanisms, this form of scattering may affect the calculated mobility; however, we neglect such effects under the (qualified) assumption[8] that such corrections are indeed small.

*Electronic Mail: djena@engineering.ucsb.edu

So the treatment is best affected by neglecting localization and many-particle effects altogether, and treating electron wavefunctions as extended single particle Bloch states. Hence, transport is treated in the traditional regime of the Born-approximation. Scattering rate from a state $|k>$ to a state $|k'>$ is evaluated using Fermi's Golden Rule,

$$S(k,k') = \frac{2\pi}{\hbar}|H_{kk'}|^2\delta(E_{k'} - E_k) \tag{1}$$

where $\hbar$ is the reduced Planck's constant, $H_{kk'} =< k'|V(r)|k > \cdot I_{kk'}$ is the product of the matrix element $< k'|V(r)|k >$ of the scattering potential $V(r)$ between plane wave states $< r|k >= 1/\sqrt{A}e^{ik_\perp r_\perp}\chi(z)$ and the matrix element $I_{kk'}$ between lattice-periodic Bloch functions. Owing to the wide bandgap of the nitrides, the matrix element $I_{kk'} \approx 1$, the approximation holding good even if there are large non-parabolicities in the dispersion[9].

Once the matrix element is determined for different forms of scatterers, transport scattering time is evaluated by summing over all the available final states

$$\frac{1}{\tau(k)} = N_{2D}\Sigma_{k'}S(k',k)(1 - \frac{\mathbf{k'}\cdot\mathbf{k}}{|k|^2}). \tag{2}$$

where N_{2D} is the total number of scatterers in the 2D area A. Converting the summation to an integral over the quasi-continuous wavevector states and exploiting the degenerate nature of the carriers for averaging $\tau(k)$ (all electrons carrying current have energy $E \approx E_F$), the measurable transport scattering rate τ reduces to the simple form[10]

$$\frac{1}{\tau} = n_{2D}^{imp}\frac{m^*}{2\pi\hbar^3 k_F^3}\int_0^{2k_F}|V(q)|^2\frac{q^2}{\sqrt{1-(\frac{q}{2k_F})^2}} \tag{3}$$

where $n_{2D}^{imp} = N_{2D}/A$ is the areal density of scatterers, m^* is the conduction band electron effective mass, $k_F = \sqrt{2\pi n_{2D}}$ is the Fermi wavevector, n_{2D} being the 2DEG density. Also, $V(q) = V_0(q)F_{nm}(q)$, where $V_0(q) =< k'|V(r)|k > /\epsilon_{2D}(q)$ is the screened matrix element for a perfect 2DEG ($|\chi(z)|^2 = \delta(z)$), and $F_{nm}(q)$ is a form factor that takes the finite extent of the realistic 2DEG along the z direction into account. For low temperature transport in the lowest subband (the electric quantum limit), we denote the form factor by $F_{11}(q) = P_0$.

For accurate evaluation of scattering rates, the finite extent of the 2DEG along the z direction must be accounted for. The exact nature of the spatial extent can be evaluated from a self-consistent solution of Schrodinger and Poisson equations using the charge control model for the device structure. Such a solution is shown in Figure 1 for an $Al_{0.27}Ga_{0.73}N/GaN$ 2DEG[11]. However, for analytic evaluation of scattering rates, the Fang-Howard variational wavefunction is a better candidate, and has been used successfully for transport calculations in the past. The form of the function is

$$\chi(z) = 0, z < 0$$
$$\chi(z) = \sqrt{\frac{b^3}{2}}ze^{-\frac{bz}{2}}, z \geq 0. \tag{4}$$

where b is a variational parameter. The parameter is chosen such that it minimizes the energy[10]; this is achieved when $b = (33m^*e^2n_{2D}/8\hbar^2\epsilon)^{1/3}$, where the sybols have their usual meaning. This form of the wavefunction leads to a form factor

$$P_0 = \eta^3 = (\frac{b}{b+q})^3 \tag{5}$$

for transport in the electric quantum limit. Screening by free carriers in the 2DEG is also affected due to the finite extent. This is reflected in another form factor $G(q)$ entering the long-wavelength ($q \to 0$) 2D dielectric function $\epsilon_{2D}(q) = 1 + \frac{q_{TF}}{q}G(q)$. Here $G(q) = \frac{1}{8}(2\eta^3 + 3\eta^2 + 3\eta)$[12], and q_{TF} is the Thomas-Fermi wavevector. For a perfect 2DEG, $\eta \to 1$, and both form factors reduce to unity.

III. DEFECTS AND SCATTERING SOURCES

Transport theory relies on the accurate identification of defects that lead to scattering of conduction electrons. Transport in AlGaAs/GaAs 2DEGs is well understood. The list of scattering sources comprises of *ionized impurities*,

interface roughness at the AlGaAs/GaAs barrier, *alloy scattering* due to penetration of the 2DEG wavefunction into the barrier, and *phonons*. In AlGaN/GaN 2DEGs, all these scattering mechanisms are present, in addition to some others. Charged dislocations and charged surface donors are the new defects, and their effects on transport for 2DEGs have received little attention.

We find the scattering rates arising out of these new defects as well as the traditional defects for the AlGaN/GaN 2DEGs. Realistic values of impurity concentrations specific to AlGaN/GaN samples got from experimental characterization techniques are incorporated in the analysis.

A. Dislocations

Due to the large lattice mismatch of GaN with the substrates on which it is epitaxially grown (SiC and Sapphire), $N_{disl} = 1 - 100 \times 10^8/cm^2$ dislocations are typically formed. These dislocations originate from the nucleation layer at the interface of the substrate and GaN, growing up to the surface without termination. The dislocations are observed to grow along the (0001) direction, piercing through interfaces.

The model used for the electrical nature of dislocations to study it's effect on transport is that of a charged line - the dislocation is modeled as a line of dangling bonds, which introduce states in the energy gap. The dangling bonds are separated by a lattice constant c_0 along the (0001) direction. This model was introduced by Read and Shockley[13], and has been successful in explaining electron mobility in bulk semiconductors, including GaN. The lineal charge density is given by $\rho_L = ef/c_0$, where e is the electron charge, and f is the occupancy number for each available site.

There has been some controversy regarding the electrical activity of dislocations, as well as for the value of the occupation function f, given that dislocations are charged. Through scanning capacitance microscopy measurements, Hansen *et. al.*[14] showed that dislocations in GaN are electrically charged. Brazel *et. al.*[15] and recently, Hsu *et. al.*[16] have shown that dislocations offer highly preferential localized current paths. Additionally, Kozodoy *et. al.*[17] showed a direct relationship of reverse leakage currents in GaN junction diodes to the number of dislocations. Schaadt *et al*[18] confirm the notion of charged dislocations from their scanning capacitance voltage measurements, and are also able to predict the amount of charge on the dislocations and the screening lengths around the charged lines.

Hence, experimental evidence strongly suggests that dislocations introduce states in band gap. However, the controversy has been in theoretical studies. Elsner *et. al.* calculated from both ab initio local density functional methods and density functional tight binding methods[19] for both pure edge and pure screw type dislocations. For screw type dislocations, the authors found deep states in the bandgap. They found no deep states in the gap for pure edge type dislocations. Calculations of Wright and Furthmüller[20] and Wright and Grossner[21], however, show that for both AlN and GaN, edge dislocations introduce electronic states in the gap. Leung *et. al.*[22] did an energetics study of the occupation probabilities for the states introduced by threading edge dislocations, drawing upon the theoretical results of Wright *et. al.*. They find that electronic states introduced in the bandgap by threading edge dislocations can be multiply occupied, and the probability of occupation of sites is a function of the background doping density.

Scattering by charged dislocations in bulk semiconductors has been treated by several authors[23], including for GaN[24,25]. However, scattering by dislocations for reduced dimensional electron systems had not been analyzed until recently[26]. We recently derived the scattering rates for a perfect two-dimensional electron gas (i.e., with zero spatial extent in the z-direction) for charged threading edge dislocations. We derive scattering rates in this work for a realistic two-dimensional electron gas with a finite spatial distribution in the z-direction. Figure 2 captures the essential model for the problem.

For simplicity, we assume the dielectric constants in the barrier and GaN to be same $\epsilon_b(AlGaN) \approx \epsilon_b(GaN) = \epsilon$. The dislocation line charge is written as $\rho_L = ef/c_0$, where e is the electron charge, c_0 is the lattice constant in GaN along the (0001) direction, and f is the fraction of occupied acceptor states introduced by the dislocation. The Fourier transform of the screened potential experienced by the 2DEG due to a differential charge element $dQ = \rho_L dz$ located a distance z away from the interface is given by[12]

$$dU(q) = \frac{e\rho_L}{2\epsilon} \frac{P_0 e^{-qz} dz}{q + q_{TF} G(q)}. \tag{6}$$

P_0 and $G(q)$ were introduced earlier. q_{TF} is the Thomas-Fermi screening wavevector for 2D systems, given by $q_{TF} = 2/a_B^*$, a_B^* being the effective Bohr radius in 2D. The total potential seen at the 2DEG is got by summing potentials of all differential elements,

$$V(q) = \frac{e\rho_L}{2\epsilon} \frac{2P_0}{q + q_{TF} G(q)}. \tag{7}$$

The scattering rate is evaluated by using Equation [3] as

$$\frac{1}{\tau_{disl}} = N_{dis}\frac{m^*}{2\pi\hbar^3 k_F^3}\int_0^{2k_F} dq|V(q)|^2\frac{q^2}{\sqrt{1-(\frac{q}{2k_F})^2}}. \tag{8}$$

With the substitution $u = q/2k_F$, we reduce the expression to

$$\frac{1}{\tau_{dis}} = \frac{m^* e^2 \rho_L^2 N_{dis}}{\hbar^3\epsilon^2}\frac{I(n_{2D})}{4\pi k_F^4}. \tag{9}$$

The dimensionless integral $I(n_{2D})$ depends on the 2DEG density. When $b \to \infty$ with $a = q_{TF}/2k_F$, the integral factor reduces to

$$I(a(n_{2D})) = \frac{\sqrt{1-a^2} + a^2 ln(\frac{1-\sqrt{1-a^2}}{a})}{a(1-a^2)^{\frac{3}{2}}} \tag{10}$$

which is the expression for a perfect 2DEG with no spatial extent in the z direction.

We find the assumption in previous works for bulk GaN scattering[24,26] that $f = 1$ predicts a lower low temperature mobility than the highest values reported till date. The energy calculations by Leung *et. al*[22] show that typically only $10-50\%$ of the states will be occupied ($f = 0.1-0.5$) for a background donor density of $N_d \approx 10^{16}/cm^3$ and dislocation densities in the $10^8 - 10^{10}/cm^2$ range (which is typical of high purity molecular beam epitaxy samples). Yu *et. al.*[18] reported $f = 0.5$ from their scanning capacitance-voltage measurements. This makes dislocations much more benign as scatterers than initially thought - note that f^2 appears in the denominator in the expression for mobility. Electron mobility due to scattering by charged dislocations *alone* $\mu_{disl} = e\tau_{disl}/m^*$ is shown in Figure [3] as a function of 2DEG carrier density. We show the values calculated for $f = 0.1, 0.5$, and 1. The dependence on 2DEG density is found to be $\mu_{disl} \propto n_{2D}^{1.34}$ (for a perfect 2DEG, the dependence was found to be $\mu_{disl} \propto n_{2D}^{\frac{3}{2}}$)[26]. A useful numerical formula that can be incorporated in Monte-Carlo techniques for treating dislocation scattering limited electron mobility in 2DEGs is

$$\mu_{disl} = 58667 \times (\frac{10^8}{N_{disl}}) \times (\frac{n_{2D}^{1.34}}{10^{12}}) \times (\frac{1}{f^2}) \tag{11}$$

where N_{disl}, n_{2D} are in cm^{-2}, f is the occupation function for filled states, and the mobility is in $cm^2/V\cdot s$. There is no temperature dependence, reflecting the degenerate nature of the carriers. Also, at a dislocation density of $10^9/cm^2$, the mean spacing between the dislocations is $\approx 300nm$, whereas the Fermi wavelength for a 2DEG concentration of $10^{13}/cm^2$ is $\lambda_F \approx 10nm$. This implies that there can be no interference effects in transport - thus the approximation that the scatterers are randomly distributed is a good one.

B. Ionized impurity

The spirit of the HEMT 2DEG is a spatial separation of the 2DEG from the ionized donors, thus reducing scattering and improving electron mobility. State of the art AlGaN/GaN systems have $N_{back} = 10^{16}/cm^3$ unintentional residual background donors. These donors have been detected by secondary ion mass spectroscopy (SIMS) measurements to be oxygen and silicon atoms that incorporate during the growth process. Transport scattering rate due to a homogeneous background donor density of N_{back} is given by

$$\frac{1}{\tau_{back}} = N_{back}\frac{m^*}{2\pi\hbar^3 k_F^3}(\frac{e^2}{2\epsilon})^2\int_0^{2k_F} dq\frac{P_0^2}{(q+q_{TF}G(q))^2}\frac{q}{\sqrt{1-(\frac{q}{2k_F})^2}}. \tag{12}$$

The absence of intentional modulation donors implies that there is a different source of 2DEG electrons. We point out that polarization by itself *cannot* supply electrons, since on the whole, it is charge neutral. What polarization *can* do however, is induce the transfer of electrons from any other possible source to satisfy requirements of electrochemical equilibrium. Background impurity densities cannot be the source of the 2DEG electrons since their concentration is too low for providing the high density 2DEG densities observed.

Electrons in the 2DEG for nitride heterostructures are believed to be supplied by surface donor states. The positive surface charge forms a sheet-charge dipole with the 2DEG which tries to neutralize the polarization dipole in the AlGaN layer. Rizzi *et. al.* have confirmed the presence of surface donor states from XPS measurements[27]. These

experiments confirm the suspicion that the surface states are charged, and are responsible for forming the 2DEG, as inferred from a purely charge control analysis by Ibbetson[29].

The surface donor states will form a source of scattering identical to a delta-doped remote donor layer. Thus, the transport scattering rate for the surface donors can be treated in the same way as an ordinary delta-doped donor layer. If the sheet density of such donors is N_s, and is at a distance d form the heterostructure interface (note that this is also the thickness of the AlGaN barrier), the scattering rate is given by

$$\frac{1}{\tau_r} = N_s \frac{m^*}{2\pi\hbar^3 k_F^3} (\frac{e^2}{2\epsilon})^2 \int_0^{2k_F} dq \frac{P_0^2 e^{-2q|d|}}{(q + q_{TF} G(q))^2} \frac{q^2}{\sqrt{1 - (\frac{q}{2k_F})^2}}. \tag{13}$$

C. Alloy disorder

Alloy disorder scattering originates from the randomly varying alloy potential in the barrier. This form of scattering is known to be the mobility limiting mechanism for 2DEGs confined in an alloy channel such as in InGaAs/GaAs heterostructures. In 2DEGs confined in binary compounds, alloy scattering occurs as a result of the finite penetration of the 2DEG wavefunction into the barrier; the scattering rate is given by[30]

$$\frac{1}{\tau_{alloy}} = \frac{m^* \Omega_0 (\delta V)^2 x(1-x)}{e^2 \hbar^3} \times \frac{\kappa_b P_b^2}{2} \tag{14}$$

where Ω_0 is the volume associated with each Al(Ga) atom, δV is the difference in potential by replacing a Ga atom by Al which is taken to be the conduction band offset between the AlN and GaN, $\kappa_b = 2\sqrt{2m^* \Delta E_c(x)/\hbar^2}$ is the wavevector characterizing the penetration of the wavefunction into the AlGaN barrier ($\Delta E_c(x)$ is the conduction band offset), and P_b is the integrated probability of finding the electron in the barrier. Figure 4 shows the probability P_b as a percentage.

In AlGaAs/GaAs heterostructures, this form of scattering is small, and often negligible[30]. However, in AlGaN/GaN heterostructures, the large electron effective mass, the high 2DEG density and the large alloy scattering potential all combine to make this form of scattering strong in spite of the confinement in the binary semiconductor. Figure [5] shows the alloy scattering limited electron mobility for a range of 2DEG densities and alloy compositions. The current highest mobilities reported in the AlGaN/GaN 2DEGs are highlighted, and the path to higher mobilities is clear from the plot.

D. Interface Roughness

Scattering at rough interfaces can be severe if the 2DEG density is high, since the 2DEG tends to shift closer to the interface as the density increases. Interfaces, however, can be grown nearly atomically flat by modern epitaxial growth techniques. The roughness at heterojunction interfaces has been traditionally modeled by a Gaussian autocovariance function. Scattering rate by a rough interface with a root mean square roughness height Δ and a correlation length L is given by

$$\frac{1}{\tau_{ir}} = \frac{\Delta^2 L^2 e^4 m^*}{2\epsilon^2 \hbar^3} (\frac{1}{2} n_{2D})^2 \int_0^1 du \frac{u^4 e^{-k_F^2 L^2 u^2}}{(u + G(u)\frac{q_{TF}}{2k_F})^2 \sqrt{1-u^2}} \tag{15}$$

where the integral is rendered dimensionless by the substitution $u = q/2k_F$.

Figure [6] shows how the distance of the centroid of the 2DEG distribution from the heterojunction interface for different alloy concentrations varies with the 2DEG sheet density. The dependence was calculated from the self-consistent Fang-Howard variational wavefunction. The dependence on the 2DEG density is characteristically much stronger than on alloy composition. Interface roughness scattering affects transport even in the presence of a binary barrier (i.e., absence of alloy scattering). Recently, Yulia *et. al.* reported the successful growth of AlN/GaN heterostructures, which removes alloy scattering completely[32]. In such high-density samples, the mobility is interface roughness scattering limited, and the calculated low temperature mobilities are well explained by our theory.

A large distribution of interface roughness sites can form localized states of the 2DEG instead of the extended states for high density samples; this limit was analyzed by Zhang and Singh, who proposed that in such a case, transport

will require phonon assisted hopping[31]. However, since the highest reported mobilities are for low density samples ($n_{2D} \approx 10^{12}/cm^2$) with no temperature dependence of conductivity for $T \leq 30K$, we believe that transport in the best samples is by band conduction.

Interface roughness scattering limited transport mobility has a characteristic L^{-6} dependence for 2DEGs in quantum wells (of thickness L), which can be observed by transport measurements on quantum wells of different thicknesses. An interesting feature of the III-V nitrides is that due to the unscreened polarization fields in thin epitaxial layers, there is a large band-bending inside the well even under no external bias. Hence the 2DEG samples one interface much more than the other; this acts as an in-built mechanism to restrict interface roughness effects on 2DEGs confined in thin unscreened quantum wells.

E. Phonons

Phonon scattering limits electron mobility at temperatures $T \geq 80K$ for 2DEGs. Scattering by three types of phonons are known to affect transport - by deformation potential acoustic phonons, piezoelectric acoustic phonons, and polar optical phonons.

Scattering by both types of acoustic phonons is considered elastic for all practical purposes. Scattering rates of the two types of phonons have been widely studied; we use the form of scattering rate derived for the Fang-Howard wavefunction[39].

Polar optical phonon (POP) energy for the wurtzite GaN crystal lattice is higher than other III-Vs ($\hbar\omega_{pop} = 92meV$). Scattering by polar optical phonons is highly inelastic. Treatment of scattering of electrons confined to two dimensions by polar optical phonons has proved to be a difficult problem to solve, and no satisfactory theory exists. In spite of the highly inelastic nature of polar optical phonon scattering, an approximate momentum relaxation rate in 2DEGs was derived by Gelmont, Shur, and Stroscio , which accurately explains experimental data over a wide temperature range[33]. The result (in CGS units) is given by

$$\frac{1}{\tau_{pop}} = \frac{2\pi e^2 \omega_0 m^* N_B(T) G(k_0)}{\kappa^* k_0 \hbar^2 F(y)} \tag{16}$$

Here, $k_0 = \sqrt{2m^*(\hbar\omega_{pop})/\hbar^2}$ is the polar optical phonon wavevector, N_B is the bosonic distribution function $N_B(T) = 1/(exp[\hbar\omega_{pop}/k_BT] - 1)$, and $F(y)$ is given by

$$F(y) = 1 + \frac{1 - e^{-y}}{y}, \tag{17}$$

y being the dimensionless variable $y = \pi\hbar^2 n_{2D}/m^* k_B T$. For mobility calculations at high temperatures, we use this expression.

F. Other scattering mechanisms

Unintentionally doped (UID) GaN exhibits a n-type nature. Initially, it was attributed to the formation of nitrogen vacancies. However, careful study of the energetics of formation of such vacancies by Van De Walle and Neugebauer has shown that formation of nitrogen vacancies is energetically unfavorable[35]. Zhu and Sawaki[34] derived the scattering rates by possible nitrogen vacancies and tried explaining bulk transport properties from their theoretical calculations. In light of recent revelations of little chance of formation, we choose not to include nitrogen vacancies in our analysis of electron transport. However, we point out that vacancy formation energies may be lowered around dislocations; we leave this question open for further studies. In an earlier work, we presented the theory of scattering arising from the coupling of polarization dipoles with alloy disorder[36]. Current highest mobility values are much lower than the mobility limited by dipole scattering; so we do not include that form of scattering in this work.

IV. ELECTRON MOBILITY

Armed with the scattering rates, we are in a position to relate the theoretical values to experimentally observed transport measurements. We consider low-temperature transport first.

A. Low Temperature

At low temperatures, the different scattering processes act independently; Matheissen's rule offers a simple way of combining the effect of all scatterers. Figure [7] shows a low temperature mobility ($\mu = e\tau/m^*$) map as a function of the 2DEG sheet density n_{2D}. The calculation was done with a dislocation density of $n_{2D} = 5 \times 10^8/cm^2$, $f = 0.1$, background density $n_{back} = 10^{16}/cm^3$, surface donor density $n_s = n_{2D}$ which is required from charge control, alloy composition $x = 0.09$, and interface roughness parameters L =10Å, Λ =2Å. Every source of scattering has been considered, and the relative effects are clearly visible in the plot.

Total mobility shows a characteristic maximum; at low sheet densities $n_{2D} \leq 10^{12}/cm^2$, charged impurity scattering from background donors, surface donors and dislocations limit electron mobility. Relative concentration of the particular form of charged impurity will determine which is the dominant scatterer. However, as is evident from the calculation, mobility at typical AlGaN/GaN sheet densities is limited by short range scatterers due to alloy disorder and interface roughness. In the range of 2DEG densities $n_{2D} \geq 10^{12}/cm^2$, alloy scattering or interface roughness scattering dominate, depending on the nature of the barrier. The shaded bands labeled 1 and 2 depict the present-day highest experimental values reported. Samples whose measured values lie in band 1 have alloy barriers of low alloy composition, whereas those in band 2 are for 2DEGs at AlN/GaN heterointerfaces. The importance of short range scatterers was also pointed out by Hsu and Walukiewicz in their recent work[37].

The mobility limit for $n_{2D} \geq n_{cr} = 10^{12}/cm^2$ is 'intrinsic' in the sense that removal of charged defects (dislocations, background impurities, etc) will not be useful in improving the mobility. The critical density n_{cr} can be used as a guideline for designing high mobility 2DEG structures. We predict that highest low temperature mobilities will be achieved for low density ($n_{2D} \approx n_{cr}$) 2DEGs. For the same carrier density, a barrier of AlN will have a larger mobility than an AlGaN barrier.

If carrier densities are lowered below the critical density n_{cr}, the effects of charged impurities will be visible. Reduction of carrier density in the AlGaN/GaN 2DEG is not straightforward, since the 2DEG is *not* controlled by intentional modulation doping. Gating is one way of achieving low carrier densities; another way is the growth of GaN (or low composition AlGaN) cap layers on top of the AlGaN barrier layer. Introduction of acceptors in the barrier can also be used to reduce the 2DEG density by compensation, though p-doping in the nitrides is currently not under good control, and it will open another source of scattering.

B. High temperature

At high temperatures ($T > 100K$), the approximation that various scattering processes are independent breaks down due to strong optical phonon scattering. However, since the total scattering rate is dominated by optical phonon scattering, using Matheissen's rule will not cause significant deviations from a more accurate calculation[39].

We plot the experimental mobility and carrier concentration values for a high mobility AlGaN/GaN 2DEG in Figure [8]. The sample growth specifics was reported elsewhere[9]. The theoretically calculated values of mobility are also plotted for the particular 2DEG, showing the effect of all scattering mechanisms. It is clear that the mobility (which is one of the highest reported) is limited by alloy scattering at low temperatures.

For AlGaN/GaN heterostructures that have a parallel conducting channel, the 2DEG contribution to transport mobility is masked at high temperatures by transport in the parallel channel. In such cases, it is important to note that the measured hall mobility has contributions from both the 2DEG and a parallel channel which is in general of lower mobility. The parallel channel is through low mobility 3D carriers thermally activated from unintentional donors which freeze out at low temperatures. So pure 2DEG effects can be seen only at cryogenic temperatures. This leads to the discrepancy in measured and theoretical mobility calculated for pure 2DEGs. This is evident in Figure [8] - there is an onset of parallel conduction through carriers in the parallel 3D layer. The sharp increase in measured carrier concentration is accompanied by a drop (shaded region) in measured mobility from the theoretical values, which are calculated for a pure 2DEG. Room temperature 2DEG mobilities exceeding $\mu_{300K} = 2000 cm^2/V \cdot s$ have been reported for samples in which parallel conduction is negligible, or through a high mobility channel[38]. Removal of the parallel conducting layer will help in reaching the theoretical mobility limits for 2DEGs imposed by POP scattering.

V. CONCLUSIONS

In conclusion, the insensitivity of high density AlGaN/GaN 2DEG transport to various charged impurities in general, and charged dislocations in particular was shown. The possible charge configuration of dislocation states

was extracted from experimental mobility values. Mobility limiting scattering mechanisms were determined. Alloy disorder scattering was shown to be limiting mobilities for AlGaN/GaN 2DEGs at low temperatures. Interface roughness scattering is the mobility limiting scattering mechanism for high density 2DEGs at AlN/GaN interfaces. Ways of getting around these apparent 'intrinsic' limits to achieve higher mobilities were outlined. Effect of parallel conduction at room temperature was shown to affect measured mobility and cause deviations from the theoretically predicted values.

ACKNOWLEDGMENTS

The authors acknowledge helpful discussions with W. Walukiewicz, I. B. Yaacov, P. Tavernier, M. Manfra, and A. Rizzi.

---

[1] S. Nakamura *et al.*, Appl. Phys. Lett. **70**, 1417 (1997).
[2] Y. F. Yu *et al.*, IEEE Electron Device Lett. **19**, 50 (1998).
[3] F. Bernardini, V. Fiorentini, and D. Vanderbilt, Phys. Rev. B **56**, R10 024 (1997).
[4] P. Waltereit *et. al.*, Nature **406**, 865 (2000).
[5] M. Manfra, private communication.
[6] I. P. Smorchkova *et al.*, J. Appl. Phys. **86**, 4520 (1999).
[7] K. Hirakawa and H. Sakaki Phys. Rev. B **33**, 8291 (1986).
[8] B. Y. Hu and K. Flensberg Phys. Rev. B **53**, 10072 (1996).
[9] B. M. Askerov, *Electron Transport Phenomena in Semiconductors* (World Scientific, Singapore, 1994), p.156.
[10] J. H. Davies, *The Physics of Low Dimensional Semiconductors* (Cambridge University Press, Cambridge, 1998), p.357.
[11] Self-consistent Schrödinger-Poisson solver written by G. Snider and available freely at http://www.nd.edu/∼snider.
[12] T. Ando, A. B. Fowler, and F. Stern, Rev. Mod. Phys. **54**, 437 (1982).
[13] W. T. Read, Philos. Mag., **45**, 775 (1954).
[14] P. J. Hansen *et. al.*, Appl. Phys. Lett. **72**, 2247 (1998).
[15] E. G. Brazel, M. A. Chin, and V. Narayanamurti, Appl. Phys. Lett. **74**, 2367 (1999).
[16] J. W. P. Hsu *et. al.*, Appl. Phys. Lett. **78**, 1685 (2001).
[17] P. Kozodoy *at. al.*, Appl. Phys. Lett. **73**, 975 (1998).
[18] D. M. Schaadt, E. J. Miller, E. T. Yu, and J. M. Redwing, Appl. Phys. Lett. **78**, 88 (2001).
[19] J. Elsner *et. al.*, Phys. Rev. B **58**, 12571 (1998).
[20] A. F. Wright and J. Furthmüller, Appl. Phys. Lett. **72**, 3467 (1998).
[21] A. F. Wright and U. Grossner, Appl. Phys. Lett. **73**, 2751 (1998).
[22] K. Leung, A.F. Wright, and E. B. Stechel, Appl. Phys. Lett. **74**, 2495 (1999).
[23] B. Pödör, Phys. Status Solidi, 16, K167 (1966).
[24] D. C. Look and J. R. Sizelove, Phys. Rev. Lett. **82**, 1237 (1999).
[25] N. Weimann *et al.*, J. Appl. Phys. **83**, 3656 (1998).
[26] D. Jena, A. C. Gossard, and U. K. Mishra, Appl. Phys. Lett. **76**, 1707 (2000).
[27] A. Rizzi, R. Lantier, and H. Lüth, Phys. Status Solidi a), **177**, 165 (2000).
[28] O. Ambacher *et al.*, J. Appl. Phys. **87**, 334 (2000).
[29] J. P. Ibbetson *et. al.*, Appl. Phys. Lett. **77**, 250 (2000).
[30] G. Bastard, J. H. Davies, *Wave mechanics applied to semiconductor heterostructures* (Halsted Press, New York, 1988), p.222.
[31] Y. Zhang and J. Singh, J. Appl. Phys. **85**, 587 (1999).
[32] I. P. Smorchkova *et. al.*, Appl. Phys. Lett. **77**, 3998 (2000).
[33] B. M. Gelmont, M. Shur, and M. Stroscio, J. Appl. Phys. **77**, 657 (1995).
[34] Q. Zhu and N. Sawaki, Appl. Phys. Lett. **76**, 1594 (2000).
[35] J. Neugebauer and C. G. Van de Walle, Phys. Rev. B **50**, 8067 (1994).
[36] D. Jena, A. C. Gossard, and U. K. Mishra, J. Appl. Phys. **88**, 4734 (2000).
[37] L. Hsu and W. Walukiewicz, J. Appl. Phys. **89**, 1783 (2001).
[38] R. Gaska *et. al.*, Appl. Phys. Lett. **72**, 707 (1998).
[39] W. Walukiewicz, H. E. Ruda, J. Lagowski, and H. C. Gatos, Phys. Rev. B **30**, 4571 (1984).

FIG. 1. Self consistent solution of Schrodinger and Poisson equations yields the z- part of the wavefunction of the lowest subband, $\chi(z)$. The electronic density variation, given by $\rho(z) = e|\chi(z)|^2$ is plotted along with the lowest subband energy. The difference in the slopes of the conduction band across the heterointerface is due to the sheet charge of the polarization dipole in the AlGaN layer.

FIG. 2. Model for calculation of scattering rate due to charged dislocation for a 2DEG with a finite extent along the z-direction. The thick line depicts the uniformly charged dislocation.

FIG. 3. 2DEG mobility due to scattering by charged dislocation lines alone. On the left is shown the dependence of mobility on the 2DEG sheet density at a fixed dislocation density, on the right is the dependence on the dislocation density at a fixed 2DEG sheet density. Plots for three distinct f values is given to highlight the sensitivity of scattering to the occupation function for dislocation introduced states in the gap.

FIG. 4. Integrated probability of the wavefunction penetration in to the AlGaN barrier as a percentage. The probability can be as high as 10% for typical AlGaN/GaN structures. Note that the penetration is reduced strongly with increasing Al composition, owing to the increase in the barrier height.

FIG. 5. 2DEG mobility limited by alloy scattering alone. Since alloy scattering is sensitive to 2DEG density n_{2D} and the alloy composition, the 2D surface shows the required compositions and densities to reduce the effect of alloy scattering in AlGaN/GaN 2DEGs. Note that the flat surface on the top is not a mobility limit, but a cutoff for the plot. The figure should serve as a useful guideline for a achieving higher low temperature mobilities in the AlGaN/GaN 2DEGs, since the current highest mobilities are alloy scattering limited.

FIG. 6. Distance of the centroid of the charge distribution from the heterojunction for three alloy compositions. The 2DEG moves closer to the interface as the density increases. The dependence on the alloy composition is weak for the same 2DEG density. For $n_{2D} \geq 10^{13}/cm^2$, the 2DEG is very close to the interface, and interface roughness scattering is very severe.

FIG. 7. Low temperature mobility with contributions from all defects, impurities, disorder, as well as by acoustic phonons at $T = 1K$. Two distinct regions are shaded - labeled 1 and 2 with circles. Region 1 is where the highest mobilities achieved till date with AlGaN/GaN samples. Region 2 is the same, but for AlN/GaN samples. Note that the mobility limits are intrinsic, and the only way to increase the mobility in each case is to reduce the 2DEG sheet density.

FIG. 8. Temperature dependence of mobility is shown. The circles indicate the mobility and 2DEG sheet density measured for a sample with one of the highest electron mobilities achieved till date. The lines (solid and dotted) are theoretical calculations. Note the deviation of experimental values from theoretical calculations at $T \geq 40K$ is accompanied by a sharp increase in measured charge density, indicating the onset of conduction through the unintentionally doped bulk, which leads to a drop of measured mobility.

This figure "2figs.jpg" is available in "jpg" format from:

http://arxiv.org/ps/cond-mat/0103461v1

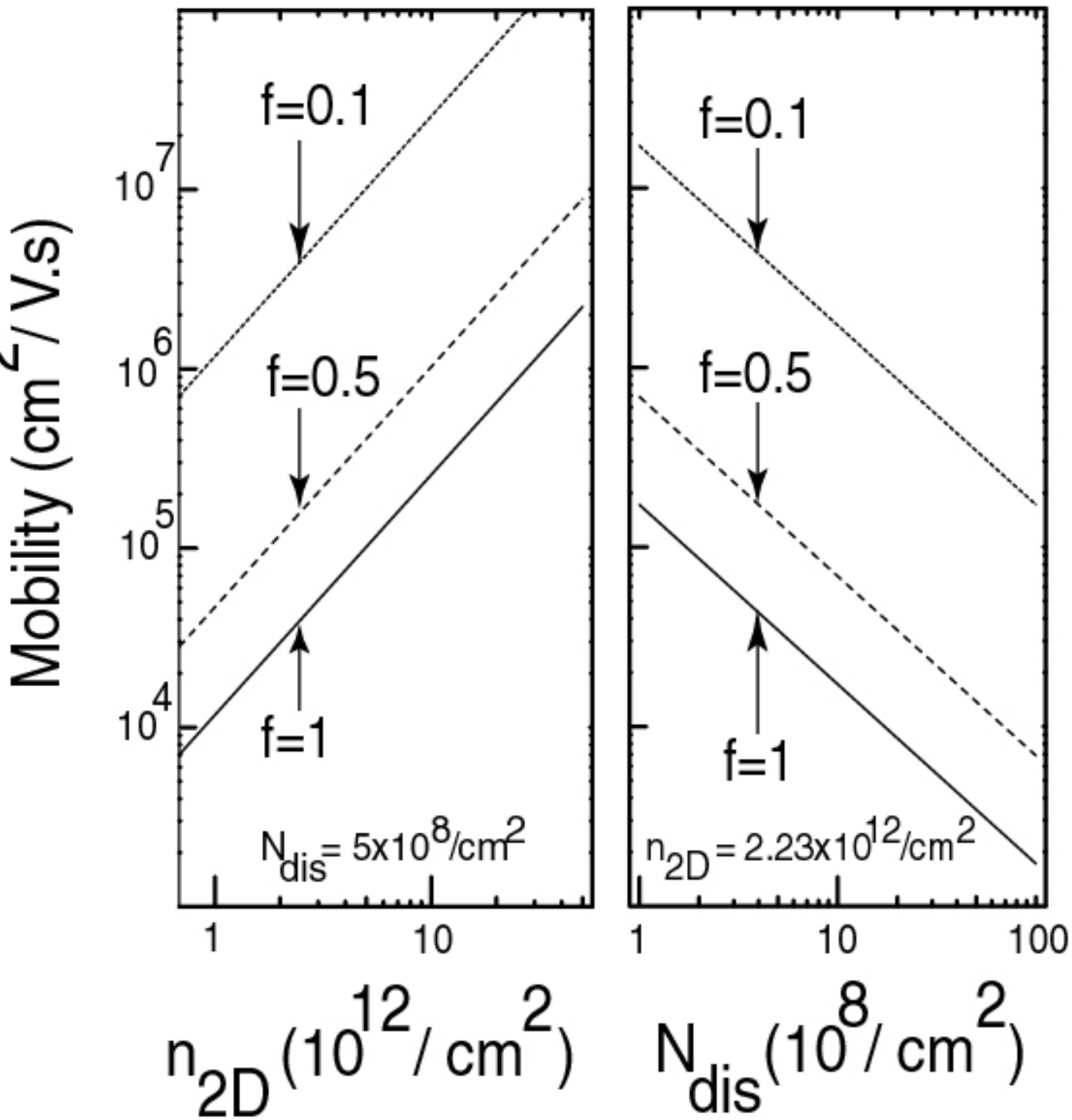
Mobility (cm^2/ V.s)
10^7
10^6
10^5
10^4
f=0.1
f=0.5
f=1
N_{dis}= 5x10^8/cm^2
1
10
n_{2D} (10^{12}/ cm^2)
f=0.1
f=0.5
f=1
n_{2D}= 2.23x10^{12}/cm^2
1
10
100
N_{dis} (10^8/ cm^2)

This figure "IR_centroid.jpg" is available in "jpg" format from:

http://arxiv.org/ps/cond-mat/0103461v1

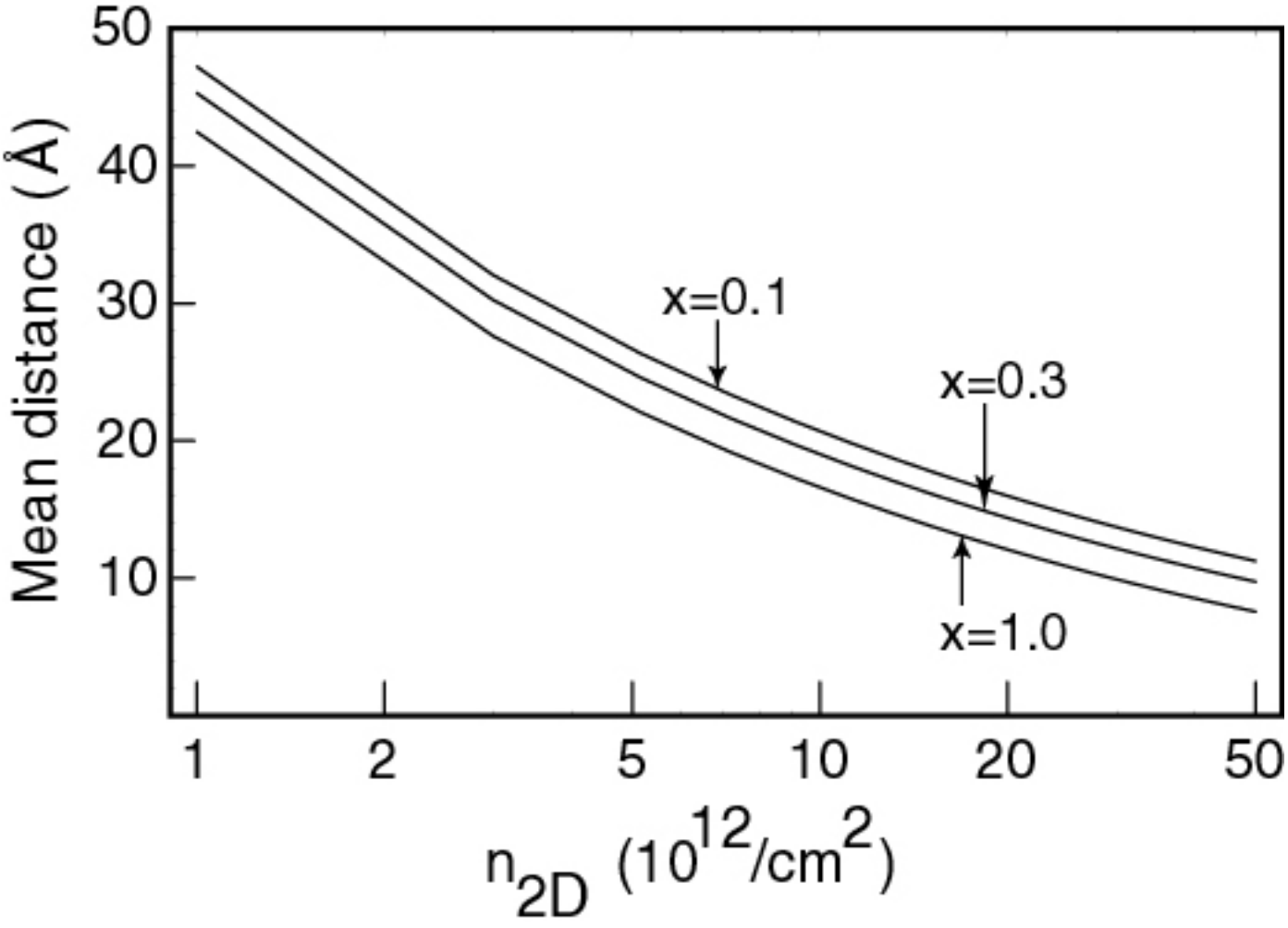
50
40
30
20
10
Mean distance (Å)
x=0.1
x=0.3
x=1.0
1
2
5
10
20
50
n2D (10^12/cm^2)

This figure "Pb.jpg" is available in "jpg" format from:

http://arxiv.org/ps/cond-mat/0103461v1

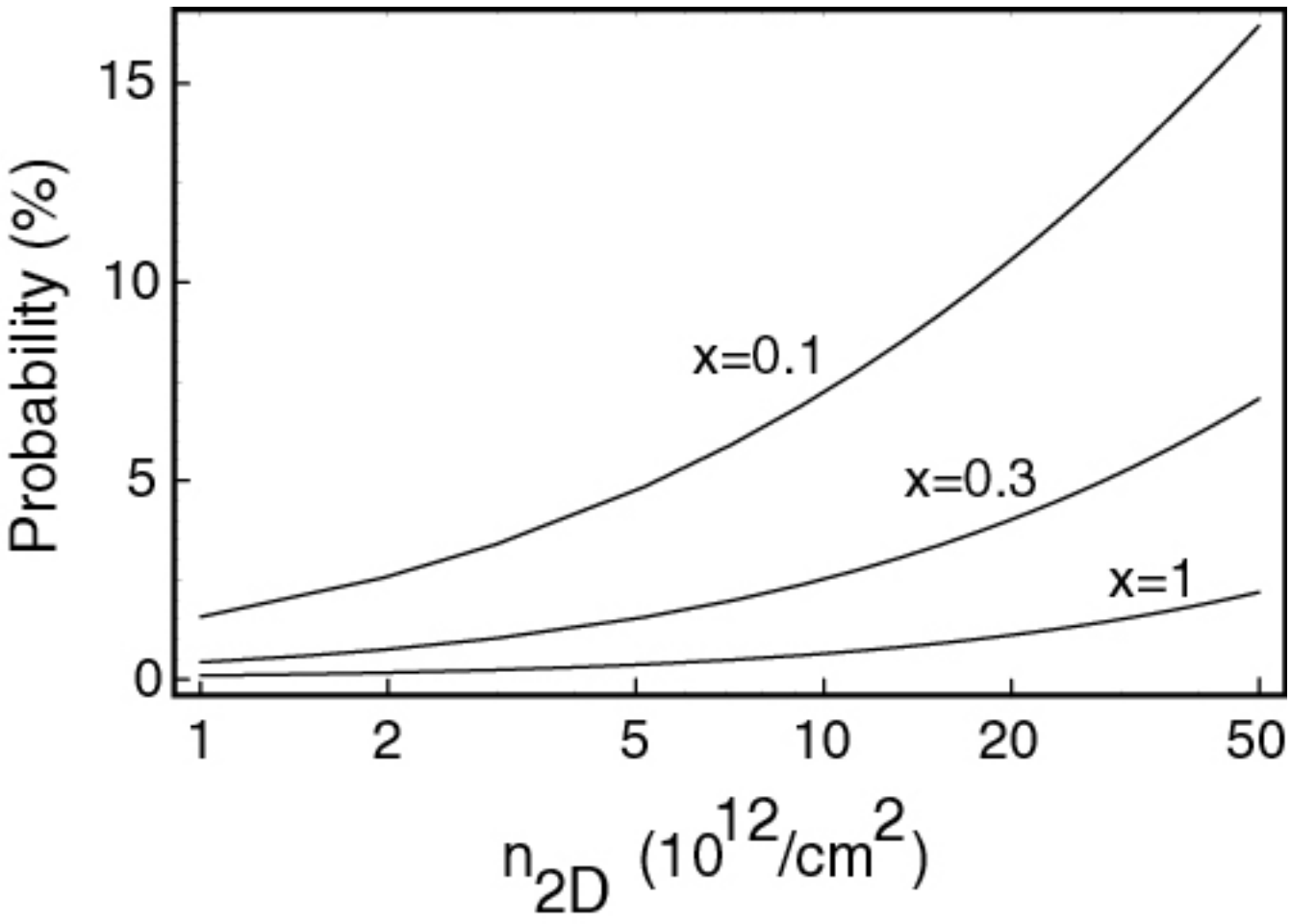
Probability (%)
15
10
5
0
x=0.1
x=0.3
x=1
1
2
5
10
20
50
n2D (10^12/cm^2)

This figure "alloy_mu.jpg" is available in "jpg" format from:

http://arxiv.org/ps/cond-mat/0103461v1

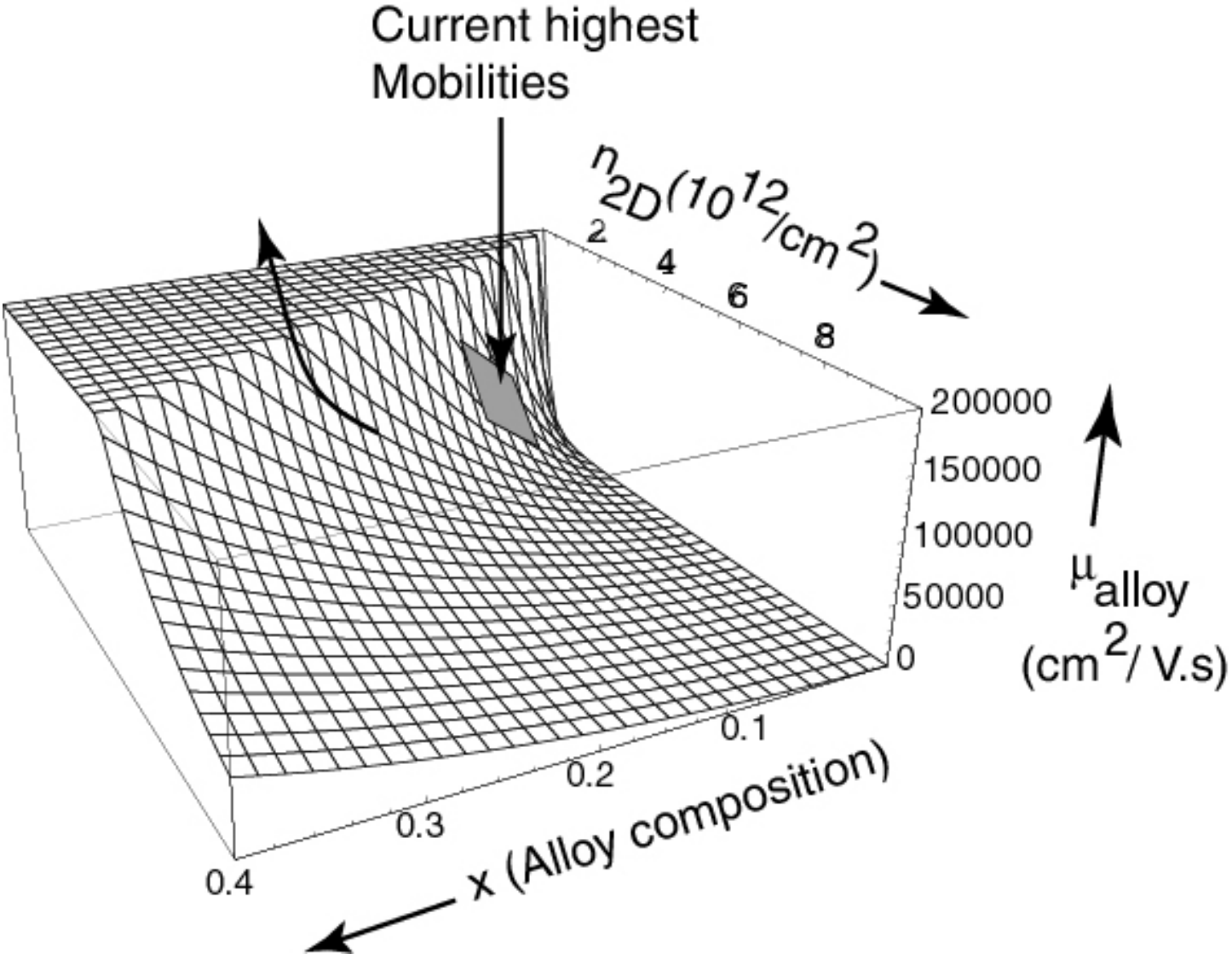
Current highest
Mobilities
$n_{2D}(10^{12}/cm^2)$
2
4
6
8
200000
150000
100000
50000
0
μ_{alloy}
$(cm^2/V.s)$
0.1
0.2
0.3
0.4
x (Alloy composition)

This figure "disl_fang_howard.jpg" is available in "jpg" format from:

http://arxiv.org/ps/cond-mat/0103461v1

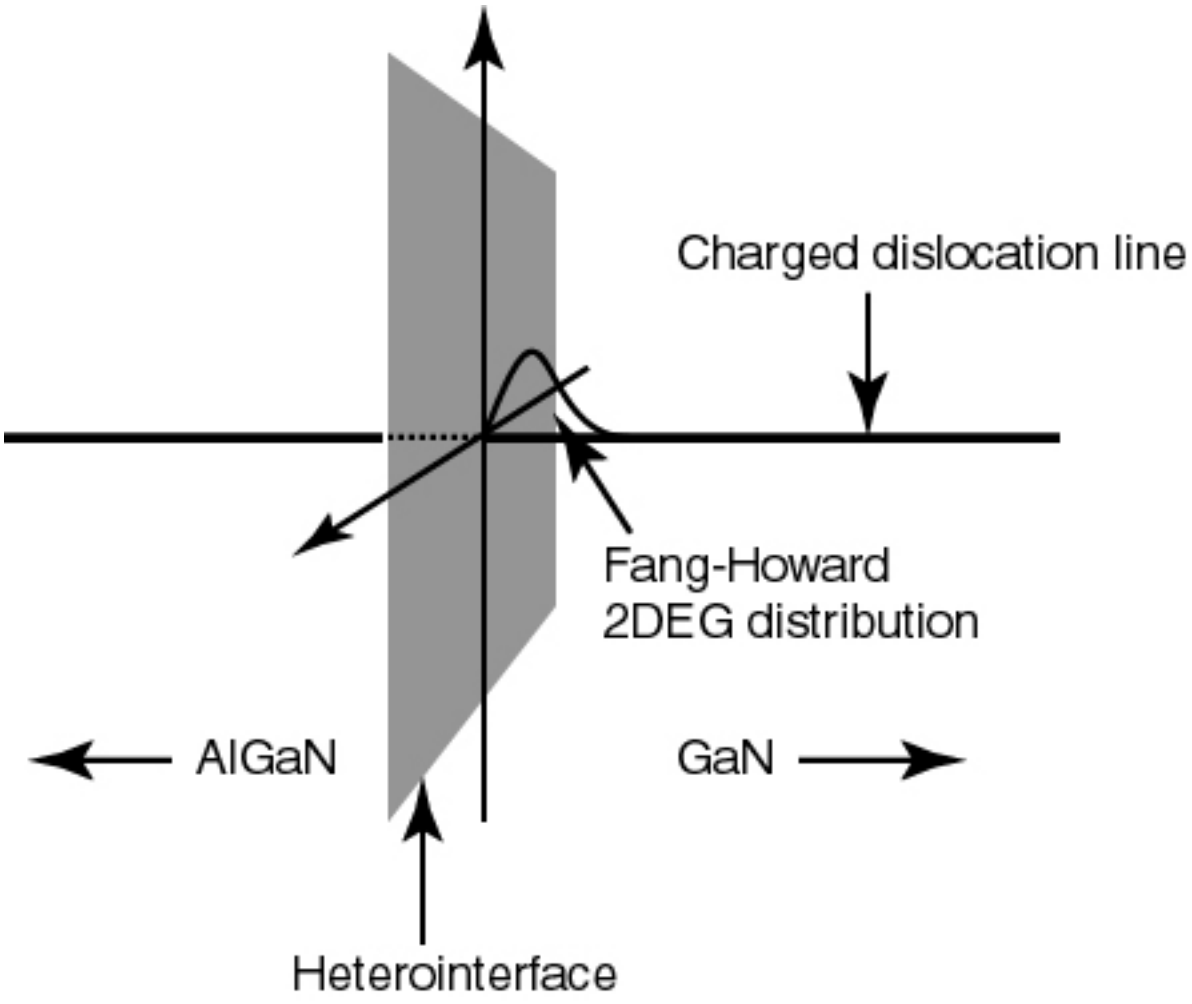
Charged dislocation line
Fang-Howard
2DEG distribution
AlGaN
GaN
Heterointerface

This figure "physrev_mu_T_theory_data.jpg" is available in "jpg" format from:

http://arxiv.org/ps/cond-mat/0103461v1

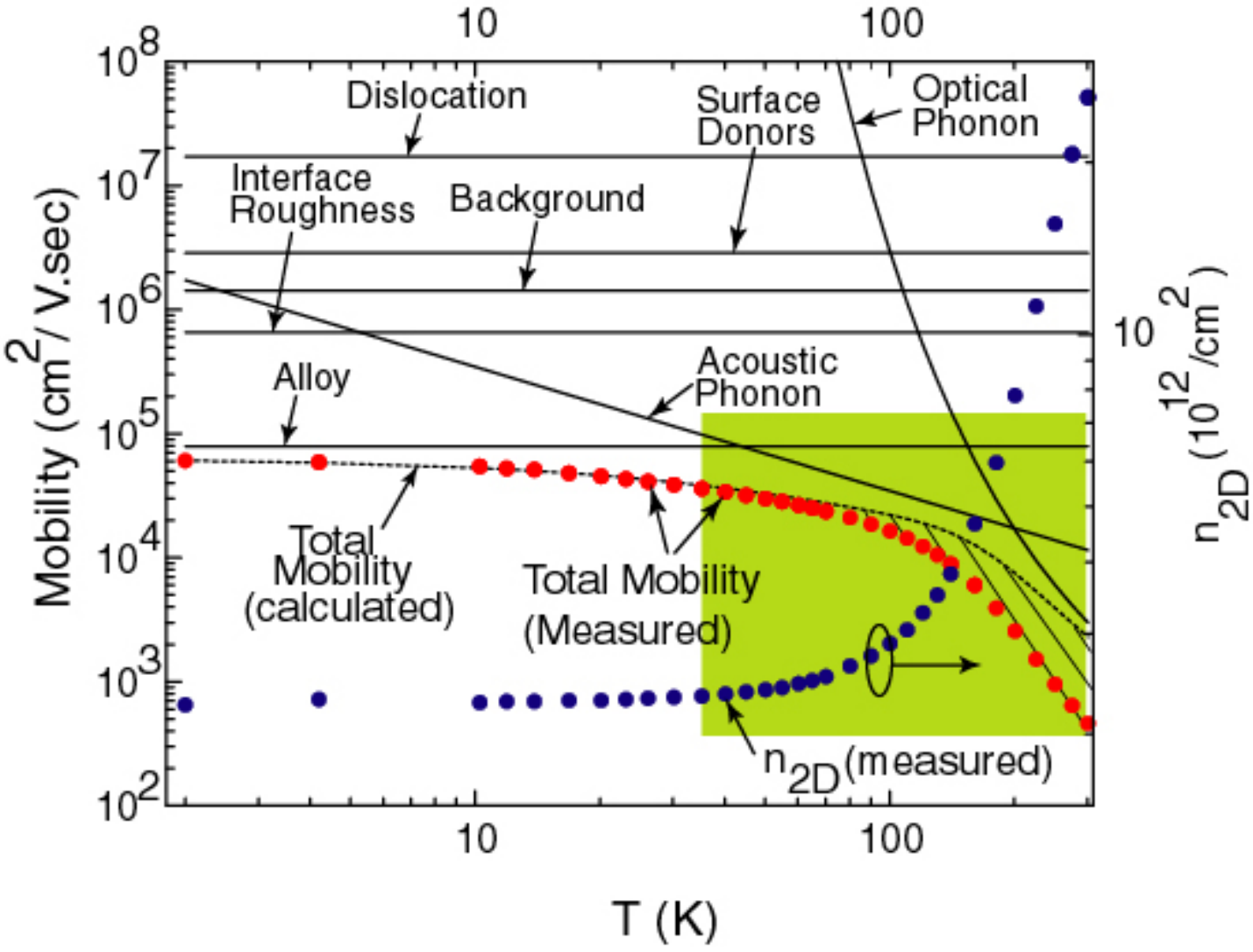
10
100
10^8
10^7
10^6
10^5
10^4
10^3
10^2
Dislocation
Surface Donors
Optical Phonon
Interface Roughness
Background
Alloy
Acoustic Phonon
Total Mobility (calculated)
Total Mobility (Measured)
n_{2D}(measured)
Mobility (cm^2/ V.sec)
n_{2D} (10^{12} /cm^2)
T (K)

This figure "physrev_mu_ns_theory_data.jpg" is available in "jpg" format from:

http://arxiv.org/ps/cond-mat/0103461v1

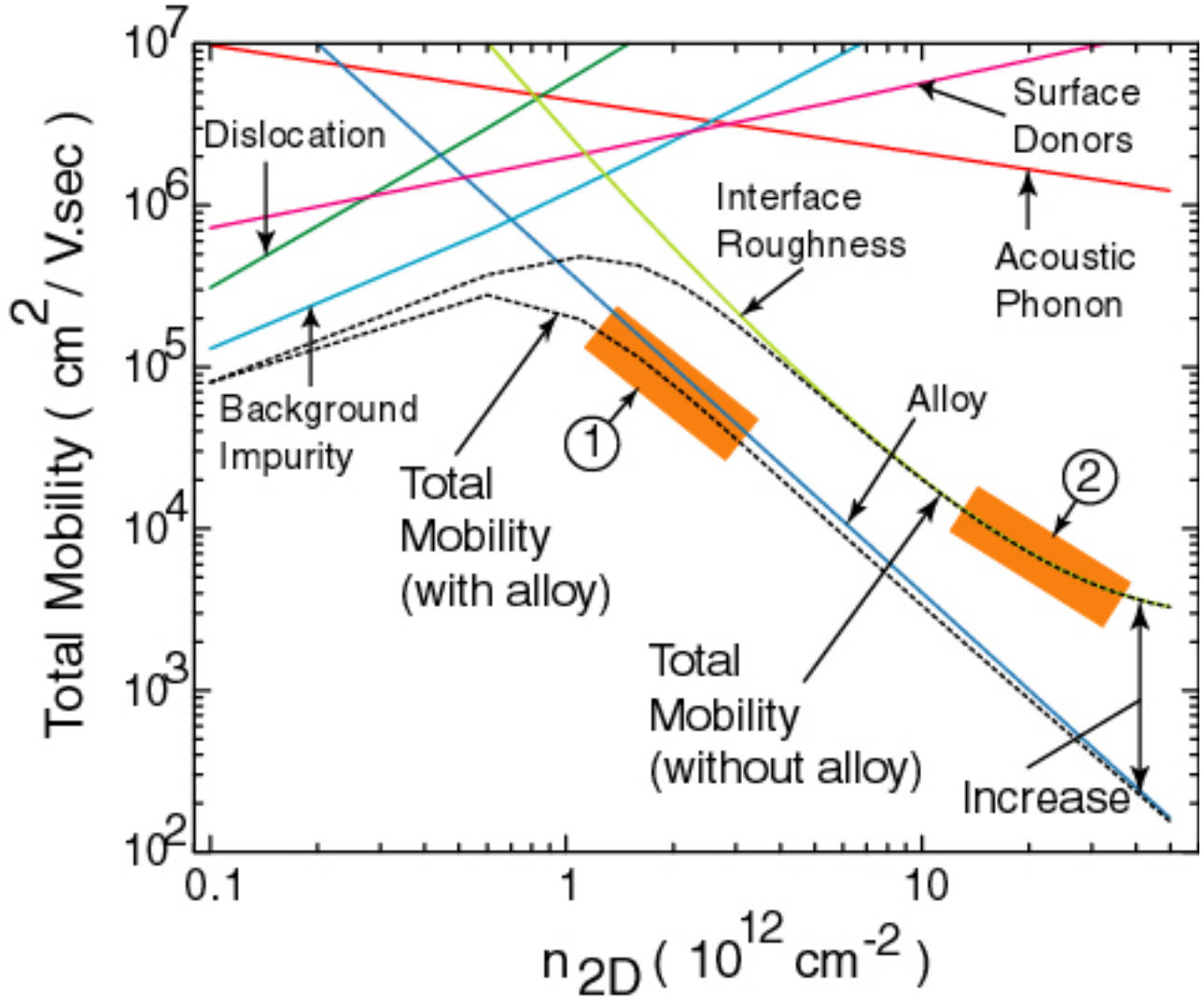
Total Mobility (cm 2 / V.sec)
10 7
10 6
10 5
10 4
10 3
10 2
0.1
1
10
n 2D (10 12 cm -2)
Dislocation
Surface
Donors
Interface
Roughness
Acoustic
Phonon
Background
Impurity
Alloy
1
2
Total
Mobility
(with alloy)
Total
Mobility
(without alloy)
Increase

This figure "wavefunc_algan_gan_2deg.jpg" is available in "jpg" format from:

http://arxiv.org/ps/cond-mat/0103461v1

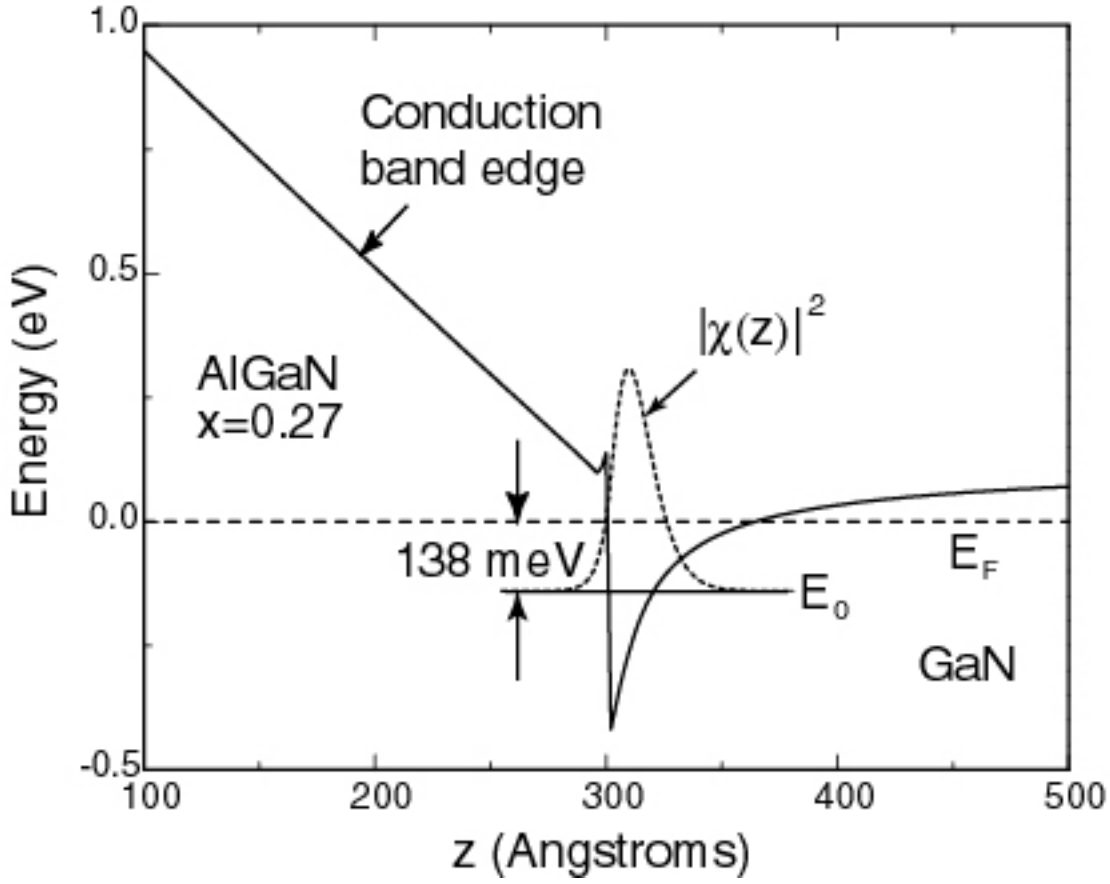
1.0
0.5
0.0
-0.5
Energy (eV)
100
200
300
400
500
z (Angstroms)
Conduction
band edge
AlGaN
x=0.27
$|\chi(z)|^2$
138 meV
E_F
E_o
GaN